Optimal Range Assignment in Solar Powered Active Wireless Sensor Networks

Benjamin Gaudette[‡], Vinay Hanumaiah[§], Sarma Vrudhula[‡] and Marwan Krunz[*]
[‡]Department of Computer Science, Arizona State University, Tempe, AZ
[§]Department of Electrical Engineering, Arizona State University, Tempe, AZ
[*]Department of Electrical and Computer Engineering, University of Arizona, Tucson, AZ
Email:{bgaudett,vinayh,vrudhula}@asu.edu, krunz@email.arizona.edu

***Abstract*—Energy harvesting in a sensor network is essential in situations where it is either difficult or not cost effective to access the network's nodes to replace the batteries. In this paper, we investigate the problems involved in controlling an active wireless sensor network that is powered both by rechargeable batteries and solar energy. The objective of this control is to maximize the network's quality of coverage (QoC), defined as the minimum number of targets that must be covered over a 24-hour period. Assuming a time varying solar profile, the problem is to optimally control the sensing range of each sensor so as to maximize the QoC. Implicit in the solution is the dynamic allocation of solar energy during the day to sensing tasks and to recharging the battery so that minimum coverage is guaranteed even during the night, when only the batteries can supply energy to the sensors. The problem turns out to be a nonlinear optimal control problem of high complexity. Exploiting the specific structure of the problem, we present a method to solve it as a series of quasiconvex (unimodal) optimization problems. The runtime of the proposed solution is 60X less than a naive method that is based on dynamic programming, while its worst-case error is less than 8%. Unlike the dynamic programming method, the proposed method is scalable to large networks consisting of hundreds of sensors and targets. This paper also offers several insights in the design of energy-harvesting networks, which result in minimum network setup cost through the determination of the optimal configuration of the number of sensors and the sampling time.**

I. Introduction

Advances in microelectronics have made it possible to produce very low cost and low power active sensors. Consequently, the deployment of a large network of active sensors over a large geographical area is now feasible, and can be used in various applications such as environmental and structural monitoring or area surveillance [1].

A desirable feature of modern sensor networks is not to require a pre-existing infrastructure, such as power lines and network cables, but instead to use chemical batteries for sensing and communications. This introduces a number of challenging problems in the management of such a network. A substantial body of research has been conducted in the area of low-power wireless sensor network (WSN) management at the physical, networking, and application layers [1]. Regardless of how energy efficient a battery-powered WSN is made, eventually the network will fail due to the limited power resource; and sensor nodes or their batteries will have to be replaced. This can be a costly procedure if the network is deployed in a harsh or adversarial environment. A solution to this problem is to use energy harvesting in conjunction with batteries. This will reduce the cost by requiring smaller batteries for some measure of performance, or equivalently improve the performance for the same cost. Some work has been done on hybridizing sensor networks to use power from both a rechargeable battery and a renewable energy source. Currently, the most promising form of renewable energy is solar. Photovoltaic panels, more commonly known as solar panels, are becoming cheaper to manufacture and are capable of providing greater energy density, thus allowing for more harvested energy [2].

Energy harvesting adds a degree of uncertainty to the task of managing the sensors (adjusting their radii, sampling intervals, etc.) due to the unpredictability of the solar profile (cloud cover, shadows of buildings, etc.). Thus, the basic problem of guaranteeing a minimum coverage of targets becomes more acute with energy harvesting. However, an optimal scheduling policy allows a designer to scale the battery and the solar panel sizes appropriately so as to minimize the network startup cost, while ensuring a minimum quality of coverage (QoC).

In this paper, we address a general version of the *target coverage* problem for a solar-powered active sensor network with a controllable (i.e. variable) sensing range. The goal is to maximize the *QoC*, which is defined as the minimum number of monitored targets at any given time. *To the best of our knowledge, this is the first work that addresses maximizing the minimum target coverage for an energy-harvesting sensor network with variable sensor radii.* The problem is formulated as a nonlinear optimal control problem, which is, in practice, hard to solve. Using several key observations, a near-optimal approximate solution can be obtained by performing a binary search over the minimum QoC, where each iteration solves a series of quasiconvex optimization problems for all time instants, while ensuring the QoC is met for that iteration. Our experimental results indicate a 60x improvement in speed for the approximate solution over an optimal dynamic programming (DP) solution, at the cost of 8% reduction in the QoC. The proposed solution method is scalable to large networks with several hundreds of sensors and targets.

The efficiency and accuracy of the solution method permits

exploration of the network's design space. In one experiment, we trade off the cost of construction of sensors with the number of sensor nodes. The results suggest that there is a unique optimal configuration of number of sensor nodes and the corresponding average radii that minimizes the cost of network startup, while guaranteeing a minimum QoC. In another experiment, we find that for certain deployment scenarios, increasing the sampling time of sensors can increase the minimum cover.

To summarize, the key contributions of this paper are as follows:

1) We introduce the concept of optimal scheduling of sensor radii in a solar-powered WSN that maximizes the minimum QoC. In our setup, power consumption is directly related to the sensors' radii.
2) The problem is formulated as a nonlinear optimal control problem. By exploiting some special characteristics of the problem, a near-optimal approximate method is provided. The problem reduces to a binary search of quasiconvex optimization problems solved over all time intervals. The search is over the minimum cover. The proposed solution outperforms the naive DP approach by a factor of 60 in computational speed, while maintaining an accuracy within 8% of the optimal solution.
3) Several design space exploration experiments are described which offer new insights in the design and deployment of sensor networks with energy-harvesting capability.

II. Related Work

The *Operational Range Assignment Problem* for solar powered sensor networks is a general version of the target cover problem, which takes advantage of predictable renewable energy sources [3]. The simplest form of the operational range assignment problem is the cover problem. One of the most intuitive definitions of the cover problem was provided informally by Klee and solved by Chvatal [4]. Klee referred to this as the Art Gallery Problem, which can be stated as follows. Given a floor plan of an art gallery, we need to find the minimum number of stationary guards who are needed to monitor every exhibit in the art gallery, assuming that guards have a known field of vision. This was optimally solved in 2D space [5].

The cover problem has been greatly extended and modified from its original form. In sensor networks, sensor nodes ("guards") and monitored targets("art exhibits") are assumed to have fixed locations at a given time. Therefore, we need to find a subset of these nodes such that all targets are covered. In the case where all sensors have a fixed sensing radius, full cover verification can be determined efficiently through the use of techniques like binary decision diagrams [6] and perimeter cover methods [7].

By considering the limited energy supply of sensor nodes, the cover problem extends to the cover lifetime problem. The goal of this problem is to extend the period in which all targets are covered. This is typically addressed by minimizing the total energy consumption [8], [9] or by prolonging the lifetime of the weakest node [6].

In [3], the lifetime problem was extended further by introducing multiple discrete sensing ranges, which sensors may choose from at any given time. We refer to this problem as the *operational range assignment problem* (ORAP). The authors have shown that the ORAP is NP-Complete, and have provided several heuristics and approximations for it. One approximation is based on a centralized linear programming (LP) approach, which finds a series of valid covers that maximize the network lifetime. Another approximate solution uses a greedy heuristic, whereby covers are constructed by sequentially increasing a node's sensing radius until the maximum number of targets is covered. The results produced by this method were found inferior to the LP solution, because the constructed covers require a wide variation in sensing ranges among nodes. Although this method is valid for a linear sensor power model, in realistic scenarios, where the required power consumption increases at least quadratically with sensor radii, it is not applicable.

The solution from [3] was improved with the addition of fuzzy sensor location knowledge. In [10]. The proposed solution used a distributed approach to solve the ORAP similar to the greedy method used in [3]. The approach in [10] consists of two phases. In the first phase, sensors increase their radii in the order of their remaining battery lifetimes until all targets are covered. In the second phase, radii are decreased, while ensuring that full coverage is still met. Although this method increases the network lifetimes substantially, it does not incorporate energy harvesting.

There has been some focus on increasing network lifetime through message routing in solar-powered networks. Niyato et. al. [11] explored the unpredictability of energy harvesting via solar radiation. With the use of Markovian models and game theory, cooperation between sensors was established to minimize losses in message passing, and thus, increasing the overall energy efficiency of the network. In [12], a set of routing protocols for battery powered WSNs was introduced, with the goal of avoiding message routing through areas of the network with reduced solar energy. A gradient was formed at each sensor node, which determined the subsequent path of a message leading to the destination. Results show that there were considerable energy savings in shifting the burden away from resource-limited nodes.

III. System Models

Fig. 1 shows the setup of a typical energy-harvesting sensor node. The node consists of an energy harvesting unit (a small solar panel), a microcontroller unit, a rechargeable battery, an RF communication unit, and a radial sensor (ultrasonic, radar, etc.). The function of the energy management circuitry is to ensure proper charging and discharging of a battery. Both the solar panel and the battery can supply power to a sensor at the same time. Likewise, the solar panel may charge a battery and power the sensor node simultaneously.

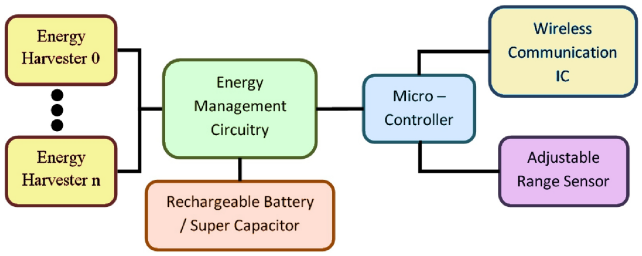

Fig. 1. Architecture of a typical energy-harvesting sensor node.

TABLE I
NOTATION

S	Set of sensor nodes and their corresponding locations
N	Number of sensor nodes
T	Set of targets and their corresponding locations
M	Number of targets.
$r_n(t)$	Radius of sensor n at time t
$B_n(t)$	Battery charge of sensor n at time t
$P_n^{sen}(r)$	Power consumption of sensor n at radius r
$P^{sol}(t)$	Power delivered by the solar panel at time t
$\zeta(\mathbf{r}(t))$	Cover function

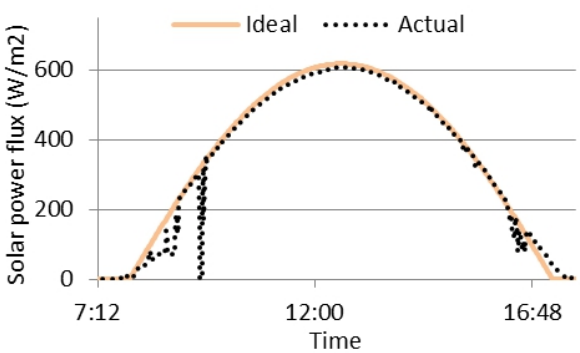

Fig. 2. Ideal and actual solar power profiles observed in Phoenix, Arizona on January, 2011 [15].

The main notation used in this paper is given in Table I. For clarity, this paper uses **bold** variables to represent vectors. Individual sensors and targets are denoted by a subscript.

A. Solar Profile

A solar profile is the power provided by the solar panel as a function of time. In practice, this profile is a random process; however, the theoretical maximum solar power profile (also called the ideal solar profile) may be modeled with the knowledge of the Sun's and Earth's physical properties (speed, rotation, shape, and so on). We use the models from [13] and [14] to characterize the ideal solar radiation. Fig. 2 shows the ideal and actual solar profiles for January 16, 2011 in Phoenix, Arizona [15]. For most of our studies, we will assume the solar profile is ideal; however, our solution is applicable to any possible solar profile. The efficiency of most modern solar panels is found to be 15% [16], and the same will be assumed in this paper.

B. Sensor Characteristics

The sensor system assumed in this work consists of active, radial-area sensors, such as ultrasonic sensors and radars. Such sensors work by transmitting data in the form of waves to detect the presence or absence of a target. If the target is present, the sensor will receive either a response from the target or the remnants of the reflected/scattered data that the sensor originally sent [17]. The relationship between the sensor's transmission power (P_r) and its received power (P_t) is given by the Friis transmission equation [18],

$$\frac{P_r}{P_t} = G_r G_t \left(\frac{\lambda}{4\pi r}\right)^{\alpha}. \tag{1}$$

G_t and G_r are the transmit and receive antenna gains, λ is the signal wavelength, α is a path-loss exponent (between 2 and 5), and r is the distance between the transmitter and the receiver. The above equation may be rearranged to find the required transmission power for a given distance and a given minimum required receive power:

$$P_n^{sen}(r) = \left(\frac{P_r^{min}}{G_r G_t}\right)\left(\frac{4\pi r}{\lambda}\right)^{\alpha}. \tag{2}$$

For dish-based radar systems, the following equation is equivalent to (2):

$$P_n^{sen}(r) = \frac{P_r^{min}(4\pi)^2 r^4}{G_r G_t A_r \sigma F^4}. \tag{3}$$

where A_r is the area of the receiver's dish, F is the propagation factor ($F = 1$ in vacuum), and σ is the scattering coefficient of the target. For simplicity, we ignore the signal interference between simultaneously active sensors, and assume that such interference is managed by the underlying MAC layer (e.g., through an appropriate TDMA or FDMA mechanism). Channel access protocols for contention resolution and interference mitigation in WSNs are readily available.

For given antenna gains, receive-power threshold, and a scattering environment, the sensor's power can generally be expressed as in (4) where α and β are based on the properties of the sensor and μ is the average power requirement of all other system components:

$$P^{sen}(r) = \beta r^{\alpha} + \mu. \tag{4}$$

Without loss of generality we assume, a given routing structure for the WSN (i.e., multi-hop paths from individual sensors to the sink are already established), where a fixed RF transmission power is used to communicate sensed data from one sensor to the next along the end-to-end path. In this case, the constant μ in (4) can be used to account for energy consumption related to channel access, data processing (e.g., fusion), and inter-sensor communications.

C. Battery Model

In this work, we use a simple linear battery model (linear charging and discharging) with no energy loss or leakage. However, our work can easily accommodate more realistic

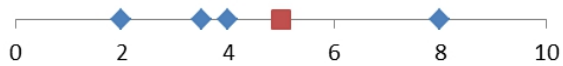

(a) 1-D sensor network. The sensor location is denoted by a square and target locations by diamonds.

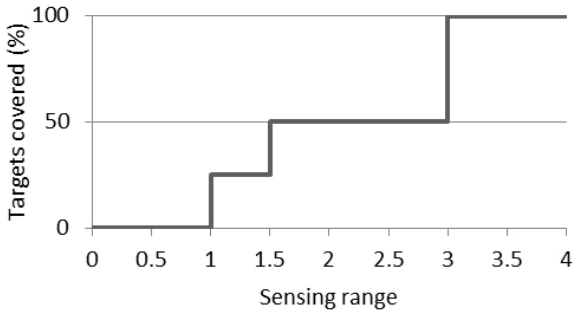

(b) The corresponding cover function.

Fig. 3. 1-D sensor network and its cover function.

models, including those that account for *rate-dependent capacity* and temperature dependence [19]–[21]. For short term operations, such as the 24-hour target monitoring application addressed in this paper, the benefits of using a more complicated battery model are negligible. As shown later, the proposed solution can work for any battery model with monotonic charging and discharging profiles. For a given sensor n, the energy in the battery at time t is given by

$$B_n(r_n, t) = B_n(0) + \int_0^t \left(P^{sol}(z) - P_n^{sen}(r_n(z))\right) dz. \quad (5)$$

D. Cover Model

A coverage model defines the fraction of covered targets as a function of the sensor radii. It depends on the locations of sensor nodes and targets. Equation (6) defines the coverage of a single target m by a single active sensor n.

$$\zeta(r_n, n, m) = \begin{cases} 0, & \text{for } r_n < 2d_{nm} \\ 1, & \text{for } r_n \geq 2d_{nm} \end{cases} \quad (6)$$

where d_{nm} is the distance between sensor n and target m. Note that the constant factor 2 comes from the sensor being an active sensor (e.g., radar), as the sensing signal travels to the target and then back to the sensor node. The total number of targets that are covered by one or more sensors in S with radii $\mathbf{r}$ is given by

$$\zeta(\mathbf{r}) = \sum_{m \in T} \max_{n \in S} \left(\zeta(r_n, n, m)\right). \quad (7)$$

Fig. 3(b) shows the cover function ζ for the 1-D sensor network in Fig. 3(a). Notice the discrete nature of the cover function w.r.t the sensor radius.

IV. The Operational Range Assignment Problem

A. Problem Description

The ORAP is defined as follows. Given a set of sensor nodes and a set of targets, find a subset of sensor nodes and their

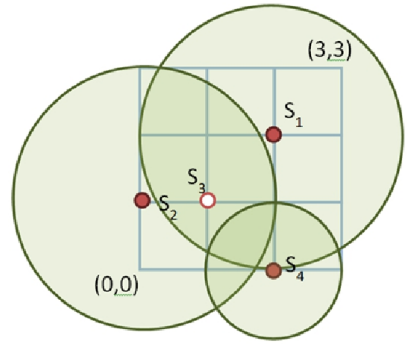

Fig. 4. An acceptable cover. Each grid point is a target.

corresponding sensing radii, which maximize the QoC for the entire operational time of the network. The QoC, which is denoted by ζ^{min}, is defined as the minimum value of $\zeta(\mathbf{r}(t))$ over the 24-hour deration. In the example in Fig. 4, a cover is found with the sensor ranges $r_1 = 2$, $r_2 = 2$, $r_3 = 0$ and $r_4 = 1$. If every point in the grid is a target, then $\zeta^{min} = \zeta(\mathbf{r}(t)) = 16$ and thus it is said to have a valid cover for $\zeta^{min} = 16$. The problem description demands such covers be computed for the entire operational time, while maximizing ζ^{min}.

The corresponding formulation is given by:

$$\max_{\mathbf{r}(t)} \quad \min_{0 \leq t \leq 24 \text{ hrs}} \quad \zeta(\mathbf{r}(t)) \quad (8)$$

$$s.t. \quad \mathbf{B}(\mathbf{r}, t) \geq \mathbf{B^{min}}, \ \forall t \in [0, 24 \text{ hours}] \quad (9)$$

$$where \quad \mathbf{B}(\mathbf{r}, t) = \mathbf{B}(0) + \int_0^t \left(P^{sol}(z) - \mathbf{P}^{sen}(\mathbf{r}(z))\right) dz \quad (10)$$

$$P_n^{sen}(r_n) = \beta r_n^{\alpha} + \mu, \ \forall n \in S. \quad (11)$$

In the above formulation, the objective (8) is to maximize the minimum level of coverage at any time during a day. The constraint (9) prevents the battery of any sensor from falling below a specific threshold, while (10) describes the charge/discharge behavior of the battery. The optimization parameter is the vector of time-varying sensor radii $\mathbf{r}(t)$. The above formulation falls under the realm of nonlinear optimal control problems [22].

Note that the sensor radii are assumed to be continuous. In practice, however, they are discrete. Hence, the radii obtained from the solution have to be discretized to correspond to the discrete set of ranges.

Nonlinear optimal control problems of the above type are typically hard to solve, computationally expensive problems. Common solution techniques are based on dynamic programming (DP) and the Hamilton-Jacobi-Bellman method [22]. To solve this problem using DP, the entire duration of execution (the 24 hour period) should be partitioned into K time intervals that approximate the continuous nature of the problem. Furthermore, discretization of the states and controls is needed. Let Q_b denote the number of states for the battery energy and let Q_r be the number of discrete values for the

sensor radii. The run time complexity of the DP solution would be $O(K(Q_b)^N(Q_r)^N)$ for an N-sensor network, since the solution requires examining all possible controls at every possible state.

We make a few novel observations, which enable us to solve the above problem using a binary search technique, where each iteration of the binary search requires the solution of K quasiconvex optimization problems for K time intervals. The details of this transformation are provided in the next section.

B. Solution Outline

We first make the following observations regarding the problem formulation (8)–(11):

1) For a fixed time, the objective function in (8) is a discrete quasilinear function in $\mathbf{r}(t)$. A quasilinear function is basically a monotonic function (weak form of convexity, also a quasiconvex function).
2) The rest of the formulation (10)–(11) can be easily shown to be convex.
3) The resulting optimized overall minimum cover ζ^{min} has to be a constant over all time instants. This is because the goal is to maximize the minimum cover over the entire duration of operation. There is no added benefit of having a higher cover over the minimum cover for any duration of time, as it does not help in maximizing the objective.

It is the last observation that is key in the transformation of the formulation. Since ζ is a constant (say ζ^{min}), we can now solve the formulation (8)–(11) as a quasiconvex optimization problem for a specified time to achieve ζ^{min} coverage. This is repeated for all K intervals to ascertain if ζ^{min} coverage is attainable. If not, ζ^{min} is lowered; otherwise, it is increased to determine the next maximum ζ^{min}. This search process of determining optimal ζ^{min} can be done through a binary search technique. Note that in the above mentioned convex optimization problem, there is no real objective, as the objective is a constant ζ^{min}. This gives rise to multiple solutions. In order to avoid this, we take the minimization of the total network energy consumption as a new objective in the above discussed convex optimization problem. Algorithm 1 outlines the problem transformation discussed in this section.

Input: $\mathbf{B}(0), P_{sol}, S, N, T, M$
Output: optimal radii schedule $\mathbf{r}^*$

1 **begin**
2 $\quad max = M$; $min = \zeta^{min,*} = 0$;
3 $\quad$ **while** $min \leq max$ **do**
4 $\quad\quad$ *failed* = false;
5 $\quad\quad \zeta^{min} = \lfloor \frac{max-min}{2} \rfloor$;
6 $\quad\quad$ **for** k = *1 to* K **do**
7 $\quad\quad\quad$ Solve the quasiconvex optimization problem to find a minimum energy cover s.t. $\zeta(\mathbf{r}(k)) \geq \zeta^{min}$ and $\mathbf{B}(k) \geq \mathbf{B^{min}}$ as described in Section V;
8 $\quad\quad\quad$ **if** *No cover found* **then**
9 $\quad\quad\quad\quad$ *failed* = true; break;
10 $\quad\quad\quad$ **end**
11 $\quad\quad\quad$ Update $\mathbf{B}(k)$;
12 $\quad\quad$ **end**
13 $\quad\quad$ **if** *failed* **then**
14 $\quad\quad\quad max = \zeta^{min} - 1$;
15 $\quad\quad$ **else**
16 $\quad\quad\quad min = \zeta^{min} + 1$;
17 $\quad\quad\quad$ **if** $\zeta^{min} > \zeta^{min,*}$ **then**
18 $\quad\quad\quad\quad \zeta^{min,*} = \zeta^{min}$; $\mathbf{r}^* = \mathbf{r}$;
19 $\quad\quad\quad$ **end**
20 $\quad\quad$ **end**
21 $\quad$ **end**
22 **end**

Algorithm 1: Solution outline to the operational range assignment problem.

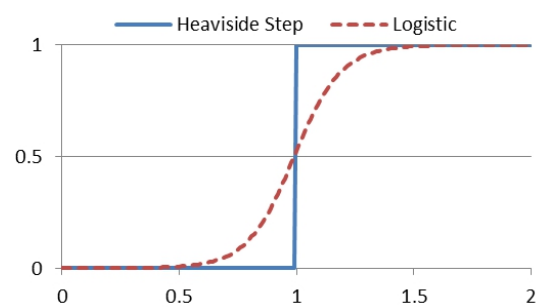

Fig. 5. The Heaviside Step function and the Logistics function.

V. Quasiconvex Optimization Solution

In this section, we discuss the details of the quasiconvex optimization formulation for the kth interval, $k \in K$,(Step 7 of Algorithm 1). We first present a continuous approximation of the discrete function ζ in (7). This is necessary as gradient-based solution techniques for convex programming require the objective and all constraints to be differentiable. Towards this, we approximate the discrete jumps in the cover function (see Fig. 3(b)) with a *Logistics* function, as shown in Fig. 5. The corresponding equations are:

$$\zeta(\mathbf{r}(k)) = \sum_{m \in T} \max_{n \in N} (L(r_n/d_{nm})) \tag{12}$$

$$where \quad L(x) = \frac{1}{1 + e^{-c \cdot x + \delta}}, \ \forall x \in (0,1) \tag{13}$$

$$\delta = \ln(1/\epsilon - 1) + c. \tag{14}$$

L is the logistics function. Since x in (13) is bounded, r_n in (12) is normalized by d_{nm}. The constants c and ϵ are quality factors, used to control how closely the logistics function resembles the step function. Increasing these values provides a better approximation, but at the cost of increased solution

TABLE II
COMMON NETWORK PARAMETER VALUES

Param	Value	Param	Value	Param	Value
r^{max}	10 m	α	3.14	Panel Size	5 cm^2
B^{ini}	0.72 kJ	β	0.0002	Area	15 m^2
B^{max}	4.32 kJ	μ	0.003	B^{min}	0 kJ
K	48				

time for the optimizer.

With this, the quasiconvex formulation for a kth interval is given by:

$$\min_{\mathbf{r}(k)} \quad \sum_{n=1}^{N} P^{sen}(r_n(k)) \tag{15}$$

$$s.t. \quad \mathbf{B}(k) = \mathbf{B}(k-1) + \int_{k-1}^{k} (P^{sol}(z) - \mathbf{P}^{sen}(\mathbf{r}(z)))\, dz \tag{16}$$

$$\mathbf{B}(k) \geq \mathbf{B}^{\mathbf{min}} \tag{17}$$

$$\zeta(\mathbf{r}(k) = \sum_{1}^{M} \max_{n \in N} (L(r_n/d_{nm})) \tag{18}$$

$$\zeta(\mathbf{r}(k)) \geq \zeta^{min} \tag{19}$$

$$L(x) = \frac{1}{1 + e^{-c \cdot x + \delta}}, \quad \delta = \ln(1/\epsilon - 1) + c \tag{20}$$

$$P_n^{sen}(r_n(k)) = \beta r_n^{\alpha}(k) + \mu, \ \forall n \in S. \tag{21}$$

The objective (15) is to minimize the total power spent by the network during each interval k. Constraint (19) requires that the minimum cover be above a specific level. The other constraints are the same as in (10)–(11), but for a given interval. It is easy to show that the above equations are convex, except for (18) and (20). Logistic functions are monotonic functions. Hence they are also quasiconvex functions [23]. Since `sum` and `max` are convex functions when their inputs are monotonic, (18) is a quasiconvex function. This makes the above formulation a quasiconvex optimization problem.

VI. SIMULATION RESULTS

A. Simulation Setup

We experimentally verify the proposed solution for the ORAP by simulating a stationary network of sensor nodes and targets in various location configurations. The default network parameter values are given in Table II. Unless noted otherwise, these values are used in all subsequent experiments. We assume that all sensor nodes are homogeneous. We use the solar profile depicted in Fig. 2. In order to highlight the benefits of our technique, network topologies were generally configured in a manner such that 100% coverage is not achievable in trivially small networks ($N < 100$).

B. Time Plots of Sample Scheduling of the Proposed Algorithm

Fig. 6 shows the plots of scheduling radii of sensors according to the proposed algorithm, the resulting battery charge, and the QoC over a course of 24 hours. The network is configured with 3 sensors and 25 targets, arranged in a random pattern, as shown in Fig. 6(a). The initial battery level for each sensor is set to 11 J. In the interest of clarity, only 3 hour of the radii schedule is shown. We observe that the algorithm switches between various covers with different radii to ensure that the energy of no battery is reduced below zero, while attaining the maximum possible QoC is attained. This can be observed at time 2:30 am when the battery of Node 2 depletes completely and Node 3 increases its sensing radius to satisfy the minimum QoC. Fig. 6(e) demonstrates that the battery primarily charges during hours of sunlight, and rapidly discharges at night, as expected. The QoC of this schedule is kept constant at 3 targets.

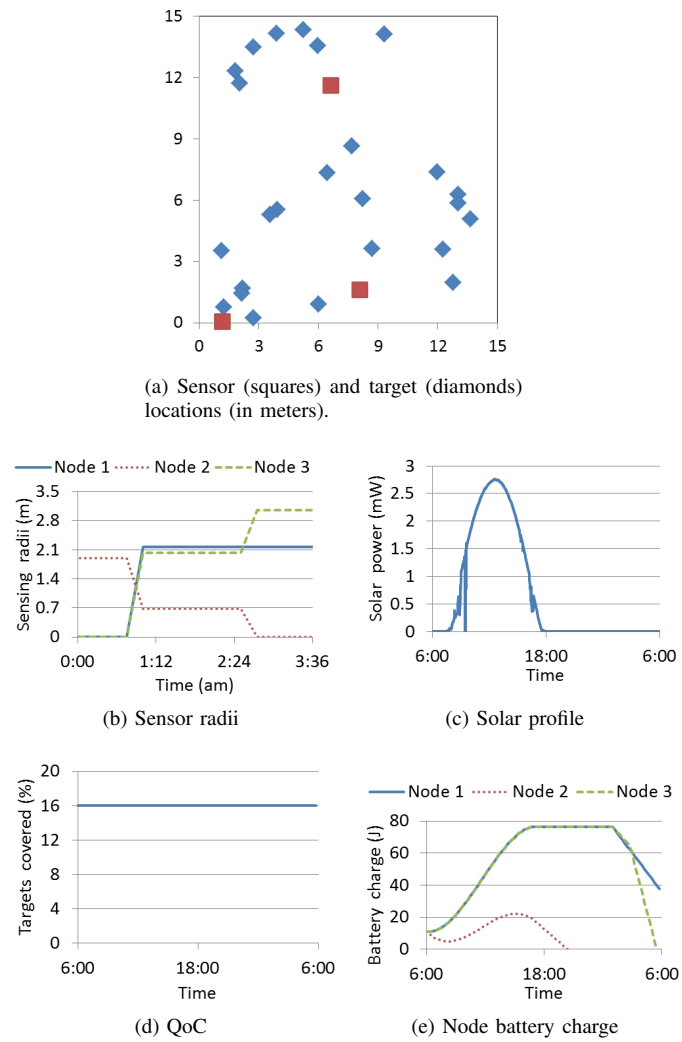

(a) Sensor (squares) and target (diamonds) locations (in meters).

(b) Sensor radii

(c) Solar profile

(d) QoC

(e) Node battery charge

Fig. 6. Time plots of scheduling for the proposed algorithm.

C. Run Time Analysis

To verify the practicality of the proposed solution, the run time of the proposed solution is compared with a dynamic programming (DP) solution. DP is one of the few known methods to solve optimal control problems; however, it re-

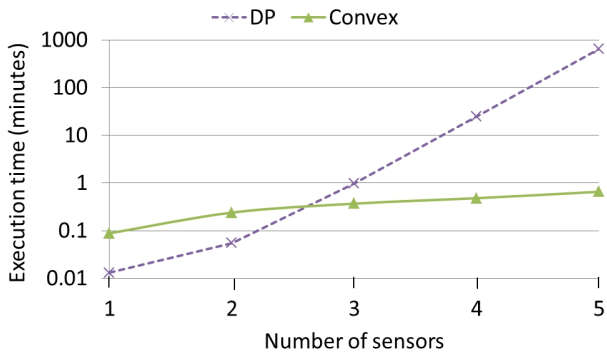

Fig. 7. Execution time vs. number of sensors.

TABLE III
RUNTIME FOR SECTION VI-C

N	1	10	20	40	50	100
Runtime	3.87 s	100 s	309 s	21.2 min	33.2 min	2.12 hr

quires all continuous variables (controls, states, time, etc.) to be discretized [22]. Increasing the number of quantized values for each of these variables will increase the accuracy of the result, but will require a longer execution time, as explained in Section IV-A. In contrast, proposed solution assumes continuous control over sensing ranges. To ensure fair comparison, the proposed algorithm is modified to choose the nearest discrete range from a set of radii used in the DP solution. This is also required for practical implementation of the proposed algorithm. All parameter values are based on existing sensor node hardware, TI's ez430-RF2500 wireless sensor node [24]. All simulations were run on a single core of a Dell workstation with a 2.93 GHz Intel core i7 and 8 GB of RAM.

In this experiment, sensors and targets were evenly distributed over the area of operation (see Fig. 8(a)). The solar profile used in the experiment is shown in Fig. 2. The maximum number of sensor nodes was limited to five, due to the enormous time complexity of the DP solution. The battery charge was quantized with 7 states and the number of sensing ranges was kept constant at 6 for the DP solution.

The results of this experiment are shown in Fig. 7. Note that the scale of the y-axis is logarithmic. We observe that as the number of senor nodes increases, the proposed solution achieves a significant speedup compared with the DP solution . Even for 4 sensor nodes, the quasiconvex optimizer finds a solution **60** times faster than the DP procedure. With such speed, one can use the proposed algorithm to explore the design space of the network in reasonable time, as seen in the subsequent experiments. Table III demonstrates that the proposed solution can handle large networks and produce solutions in reasonable time. Note that these run times are for a single-core processor. With the help of parallelization, it is possible to reduce the run times greatly.

D. Accuracy of the Proposed Solution vs. DP

The overall accuracy of the proposed solution against the naive DP solution outlined in Section VI-C is examined here. We consider three different sensor-target location configurations for this experiment as shown in Fig. 8. These configurations represent the diverse scenarios for a sensor network tasked with surveillance duty. Fig. 8(a) illustrates the case where all targets and sensors are evenly distributed across the operation area for optimal area coverage. Fig. 8(b) shows the case where all targets and sensors are evenly distributed across the area, but the sensors and the targets are separated from one another. This represents the scenario of an enemy territory surveillance. From an energy standpoint, this is one of the worst possible scenarios, as it requires larger sensing radii. Finally, Fig. 8(c) shows the case where sensors are randomly distributed. This is the most common scenario in sensor networks tasked with monitoring inaccessible areas. For these experiments, the number of battery states was increased for the DP procedure to increase its accuracy. All other parameters remained the same as in Section VI-C.

The results shown in Figs. 8(d), 8(e) and 8(f) show our proposed algorithm can cope with several possible network scenarios and provide near-optimal results. For the symmetric configuration, as N increases our proposed solution tends to provide almost identical results to the DP solution. This is due to the fact that as N increases, the mean distance from any sensor to any target decreases, thus allowing for smaller radii to be used. These smaller radii result in less energy consumption, and thus the effects of any non-ideal radii selections are reduced. For the configuration in Fig. 8(b), the two approaches gave results. This may be attributed to the fact that there are far fewer valid covers for any given ζ^{min} for this configuration as opposed to the symmetric configuration. Finally, the random configuration tends to display varying levels of error at each value of N. This is to be expected, as sensor nodes randomly positioned create vastly different network topologies. Over the results of all experiments, a peak of **8%** QoC loss was observed.

E. Effect of Number of Sensors on the Network Setup Cost

In this experiment, we study the effect of the number of sensors on the total cost of setting up a sensor network to maintain a specified QoC. The results of this experiment offer network designers with the information to trade-off number of sensors to minimize the initial setup cost of a sensor network. This is also useful to maintain an energy-neutral operation [25], which implies minimum sizing of the battery and the solar panel to reduce the operation cost, while guaranteeing a minimum QoC for a given network.

For the experiment, a large number of targets (1024) are distributed over a 200 m $\times$ 200 m area in the same fashion as in Section VI-F. The requirement is that 100% of the targets must be covered. To calculate the network setup cost, we assume that each sensor node costs \$20 [26], solar panel costs \$2 per Watt [27], and batteries cost \$0.47 per Watt-hour [28].

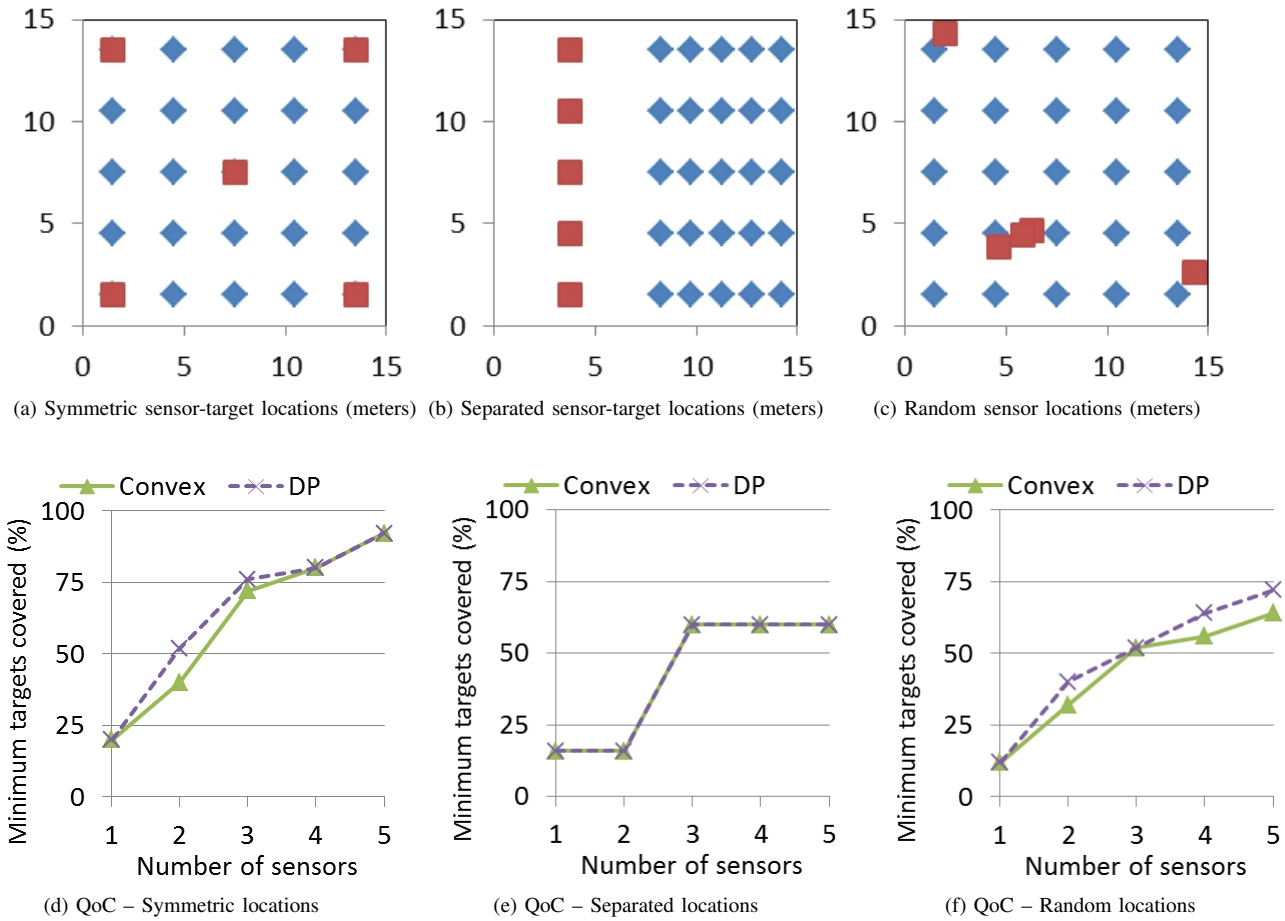

(a) Symmetric sensor-target locations (meters) (b) Separated sensor-target locations (meters) (c) Random sensor locations (meters)

(d) QoC – Symmetric locations (e) QoC – Separated locations (f) QoC – Random locations

Fig. 8. Various layout scenarios and the resulting QoC.

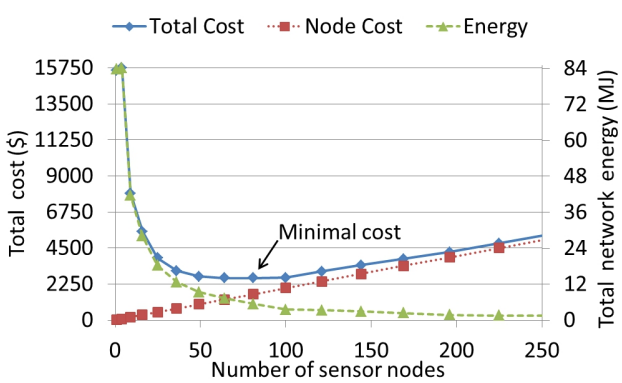

Fig. 9. Effect of number of sensor nodes on the network setup cost

With the assumption of 10 hours of sun light per day, the results shown in Fig. 9 were obtained.

Contradicting intuition, increasing the number of sensor nodes does not increase the total network energy. This is because, with more sensors, smaller radii can be used to achieve the same coverage, and the energy cost decreases at least quadratically with the radius. Because of the lower total network energy requirement, smaller batteries and solar panels are sufficient to maintain the original specified cover, thus decreasing the total network setup cost. However, an increase in the number of sensor nodes adds to the total setup cost. Thus, there exists a unique configuration of the number of sensor nodes that minimizes the overall setup cost. This is shown in Fig. 9. The plot shows a sharp initial reduction in the network energy as N increases, due to the nonlinear relation between the network energy and the sensor radii, and the fact that the effective sensor radii decreases quadratically with the increase in number of nodes.

F. Effect of the Sampling Interval on QoC

The sampling interval is the time between two consecutive sensing instants of an object. In many non-critical applications, targets do not require continuous monitoring, and for many sensor nodes continuous monitoring is impossible. For this reason, the sampling interval offers network designers a unique control variable to extend the lifetime of their networks at the expense of periods of no coverage in traditional battery powered networks. In the context of solar powered networks, the benefit is an increase in the QoC. In this experiment, the effect of reducing the sampling interval is investigated. Sensors

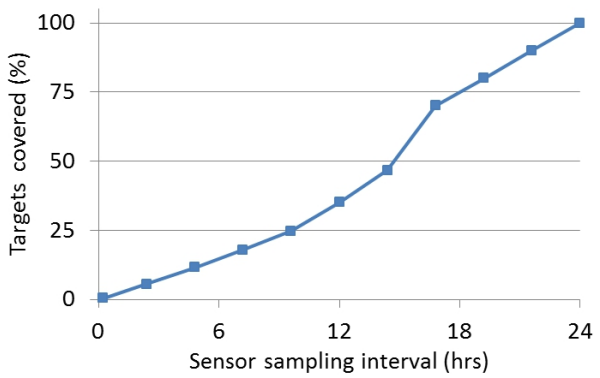

Fig. 10. Sampling interval vs. the number of sensors.

and targets are arranged in a square grid-like pattern, with equal spacing. The number of sensors was kept constant at 100 and the number of targets was kept constant at 900, deployed over a 200 m $\times$ 200 m area. The sampling interval was varied between 1% and 100% of the total operation time (the 24 hour period). We also make a slight modification to our definition of cover to be the number of targets covered averaged over the operation time.

Fig. 10 shows the result. As expected, the QoC increases with the sampling interval. This is because, increasing the sampling interval allows sensors to harvest more solar energy, and thus sensors can afford to use larger radii to enhance the QoC. It is interesting to note that initial quadratic increase in the QoC with linear increase in the sampling interval. The multiple jumps in the plot are due to the discrete nature of the cover (no. of targets) and the network topology.

VII. Conclusions

There has been a proliferation of energy-harvesting sensors in WSNs. These systems bring in additional challenges related to optimal scheduling of sensor nodes to maximize the QoC. In this paper, we presented an optimal solution to schedule active sensor nodes in solar powered networks, which maximizes the minimum attainable QoC. The proposed quasiconvex solution is demonstrated to have a large speedup compared with a naive DP solution, with minimum error in accuracy. The solution is also demonstrated to be useful in exploring the design space of energy harvesting sensor networks and the experiments provide several insights in the design of such networks.

VIII. Acknowledgements

This research was supported in part by NSF under grants CNS-0904681 and IIP-0832238. Any opinions, findings, conclusions, or recommendations expressed in this paper are those of the author(s) and do not necessarily reflect the views of the National Science Foundation.

References

[1] I. F. Akyildiz *et al.*, "Wireless sensor networks: A survey," *Computer Networks*, vol. 38, no. 4, pp. 393 – 422, 2002.

[2] P. Torcellini *et al.*, "Zero energy buildings: A critical look at the definition," in *ACEEE Summer Study*. National Renewable Energy Laboratory, 2006.

[3] M. Cardei *et al.*, "Maximum network lifetime in wireless sensor networks with adjustable sensing ranges," in *Proc. of WiMob*, vol. 3, 2005, pp. 438 – 445.

[4] V. Chvatal, ""a combinatorial theorem in plane geometry"," *Journal of Combinatorial Theory, Series B*, vol. 18, no. 1, pp. 39 – 41, 1975.

[5] J. O'Rourke, *Computational Geometry in C*. Cambridge University Press, 1998.

[6] S. Dasika, S. Vrudhula, and K. Chopra, "Algorithms for optimizing lifetime of battery powered wireless sensor networks," *Sensor Network Operations, IEEE Press*, May 2006.

[7] C.-F. Huang and Y.-C. Tseng, "The coverage problem in a wireless sensor network," in *Proc. of WSNA*. ACM, 2003, pp. 115–121.

[8] D. Diamond *et al.*, "Wireless sensor networks and chemo-/biosensing," *Chemical Reviews*, vol. 108, no. 2, pp. 652–679, 2008, pMID: 18215076.

[9] J. Yick, B. Mukherjee, and D. Ghosal, "Wireless sensor network survey," *Computer Networks*, vol. 52, pp. 2292 – 2330, 2008.

[10] O. Younis, S. Ramasubramanian, and M. Krunz, "Operational range assignemtn in sensor and actor networks," *Ad Hoc and Wireless Networks*, vol. 00, pp. 1–37, 2007.

[11] D. Niyato, E. Hossain, and A. Fallahi, "Sleep and wakeup strategies in solar-powered wireless sensor/mesh networks: Performance analysis and optimization," *IEEE Transactions on Mobile Computing*, vol. 6, pp. 221–236, 2007.

[12] T. Voigt *et al.*, "Solar-aware clustering in wireless sensor networks," *Computers and Communications*, vol. 1, pp. 238–243, 2004.

[13] J. J. Michalsky, "The astronomical almanac's algorithm for approximate solar position (1950-2050)," *Solar Energy*, vol. 40, pp. 227 – 235, 1988.

[14] "Solar position calculators," "National Renewable Energy Laboratory: Center for Renewable Energy Resources, Renewable Resource Data Center, Feb. 2000. [Online]. Available: http://www.nrel.gov/midc/solpos/

[15] "Solar Resource & Meteorological Assessment Project Southwest Solar Solar CAT, January 12, 2011 Raw Data." [Online]. Available: http://www.nrel.gov/midc/swst_solarcat/

[16] "Most efficient solar panels." [Online]. Available: http://sroeco.com/solar/most-efficient-solar-panels

[17] M. Skolnik, *Introduction to radar systems*. McGraw-Hill, 1962.

[18] H. Friis, "A note on a simple transmission formula," *Proceedings of the IRE*, vol. 34, no. 5, pp. 254 – 256, 1946.

[19] D. Rakhmatov, S. Vrudhula, and D. Wallach, "A model for battery lifetime analysis for organizing applications on a pocket computer," *IEEE Transactions on VLSI Systems*, pp. 1019–1030, December 2003.

[20] R. Rao, S. Vrudhula, and D. Rakhmatov, "Battery modeling for energy-aware system design," *IEEE Computer, Special issue on Power-Aware & Temperature-Aware Computing*, vol. 36, no. 12, pp. 77–87, December 2003.

[21] D. Rakhmatov and S. Vrudhula, "Energy management for battery-powered embedded systems," *ACM Transactions on Embedded Computing Systems*, vol. 2, no. 3, pp. 277–324, August 2003.

[22] D. Kirk, *Optimal Control Theory: An Introduction*. Englewood Cliffs, New Jersey: Prentice-Hall Inc., 1970.

[23] S. Boyd and L. Vandenberghe, *Convex Optimization*. Cambridge University Press, 2004.

[24] "ez430-rf2500 development tool user's guide (rev. e)," Texas Instruments, 2009.

[25] A. Kansal *et al.*, "Power management in energy harvesting sensor networks," *ACM Trans. Embed. Comput. Syst.*, vol. 6, 2007.

[26] "EZ430-RF2500T – MSP430 2.4-GHz Wireless Target Board." [Online]. Available: https://estore.ti.com/EZ430-RF2500T-MSP430-24-GHz-Wireless-Target-Board-P1295.aspx

[27] "Sun electronics." [Online]. Available: http://www.sunelec.com/

[28] "Battery energy: What battery provides more?" [Online]. Available: http://www.allaboutbatteries.com/Battery-Energy.html